

Electronic Supplementary Information (ESI)

**Reversible single-crystal-to-single-crystal transition in
Gd(III) metal-organic frameworks induced by heat and
solvents with a significant magnetocaloric effect**

Jin-Jin Wang, Yu Li, Teng-Fei Zheng,* Yan Peng, Jing-Lin Chen, Sui-Jun Liu*
and He-Rui Wen

School of Chemistry and Chemical Engineering, Jiangxi Provincial Key Laboratory
of Functional Molecular Materials Chemistry, Jiangxi University of Science and
Technology, Ganzhou 341000, Jiangxi Province, P.R. China

E-mail: sjliu@jxust.edu.cn (S.-J. Liu), zhengtengfei0628@163.com (T.-F. Zheng)

Materials and instrumentations

All chemical reagents were obtained from commercial sources and used without further purification. The powder X-ray diffraction (PXRD) patterns were recorded by Rigaku MiniFlex 600. The simulated PXRD patterns of single-crystal data were obtained using the Mercury software, which are freely available on the Internet at <http://www.iucr.org>. Thermogravimetric analysis (TGA) was performed under a N₂ flow at a heating rate of 10 °C min⁻¹ from 25 to 1000 °C on a NETZSCH STA2500 thermal analyzer. IR spectra in the range of 4000–400 cm⁻¹ were collected with KBr particles on a Bruker Alpha FT-IR spectrometer. Elemental analysis (C, H, and N) was performed on a vario EL cube elemental analyzer. Magnetic data were collected by a Quantum Design MPMS-XL-7 SQUID magnetometer. Diamagnetic corrections were estimated by employing Pascal constants and background corrections by experimental measurement on sample holders. DC magnetic susceptibilities were measured in temperature range of 2-300 K under a 0.1 T dc field. The plots of *M* vs *H* for **JXUST-41** and **JXUST-41a** were recorded at 2 K under the fields between 0 and 7 T. While for **JXUST-40** and **JXUST-40a**, *M* vs *H* plots were measured at the temperature range of 2-10 K under the field of 0-7 T. AC susceptibilities were performed at 2-12 K (2-7 K, 0.25 K per step; 7-12 K, 1 K per step) under a 2 kOe dc filed and 3 Oe oscillating ac filed.

Crystallographic studies for **JXUST-40**, **JXUST-40a**, **JXUST-40b**, **JXUST-41**, **JXUST-41a** and **JXUST-41b**

Single crystal X-ray diffraction data of **JXUST-40**, **JXUST-40a**, **JXUST-40b**, **JXUST-41**, **JXUST-41a** and **JXUST-41b** were recorded on a Bruker D8 QUEST diffractometer Mo-K α radiation ($\lambda = 0.71073 \text{ \AA}$) by ω scan mode. SAINT program was used for diffraction profile integration.^{S1} The SHELXT program of SHELXTL software package was used to solve the structure directly, and the full matrix least square method was used to refine the structure.^{S2} The non-hydrogen atoms were situated in successive difference Fourier syntheses and refined by anisotropic thermal parameters on *F*². Theoretically, the hydrogen atoms of BTDI⁴⁺ ligands are formed on specific atoms, and isotropic refinement was carried out by a fixed thermal factor. The

program SQUEEZE,^{S3} a part of the PLATON package of crystallographic software, was used to calculate the solvent-accessible area and remove their contributions to the overall intensity data. A solvent mask during SQUEEZE process are six water molecules for **JXUST-40a** and **JXUST-41a** based on elemental analysis and TGA. The crystal structures have been deposited at the Cambridge Crystallographic Data Center (CCDC) and allocated the deposition numbers: 230884 (**JXUST-40** at 273 K), 230885 (**JXUST-40a** at 293 K), 230886 (**JXUST-40b** at 273 K), 230887 (**JXUST-41** at 273 K), 230888 (**JXUST-41** at 293 K), 230889 (**JXUST-41b** at 273 K). A summary of the crystallographic data and refinement parameters is given in Tables S1 and S2.

References

- S1 *SAINT, Version 6.02a*, Bruker AXS Inc, Madison, WI, 2002.
- S2 G. M. Sheldrick, *Acta Crystallogr. Sect. A: Found. Adv.*, 2015, **A71**, 3-8.
- S3 A. L. Spek, *Acta Crystallogr. Sect. D-Biol. Crystallogr.* 2009, **65**, 148–155

Table S1. Crystal data and structure refinements for **JXUST-40**, **JXUST-40a** and **JXUST-40b**

Compound	JXUST-40	JXUST-40a	JXUST-40b
formula	C ₇₈ H ₅₂ N ₁₀ O ₂₈ S ₃ Gd ₄	C ₆₆ H ₄₄ N ₆ O ₃₄ S ₃ Gd ₄	C ₇₈ H ₅₂ N ₁₀ O ₂₈ S ₃ Gd ₄
<i>M_r</i>	2302.47	2190.25	2302.47
<i>T</i> (K)	273(2)	293(2)	273(2)
crystal system	triclinic	triclinic	triclinic
space group	<i>P</i> ī	<i>P</i> ī	<i>P</i> ī
<i>a</i> (Å)	10.9770(6)	11.0108(10)	10.9670(6)
<i>b</i> (Å)	11.9536(7)	11.1168(10)	11.1536(7)
<i>c</i> (Å)	15.8824(10)	15.8231(14)	15.9824(10)
<i>α</i> (°)	73.776(2)	104.973(3)	73.676(2)
<i>β</i> (°)	70.816(2)	109.460(3)	71.786(2)
<i>γ</i> (°)	86.974(2)	90.221(3)	86.984(2)
<i>V</i> (Å ³)	1888.20(19)	1755.6(3)	1780.85(19)
<i>Z</i>	1	1	1
<i>F</i> (000)	1118	1058	1118
<i>D</i> _{calc} (g cm ⁻³)	2.025	2.072	2.147
<i>μ</i> (mm ⁻¹)	3.645	3.919	3.865
Collected reflections	23531	19408	22729
Unique reflections	6575	6112	6234
<i>R</i> _{int}	0.0538	0.0685	0.0514
<i>R</i> ₁ ^a / <i>wR</i> ₂ ^b [<i>I</i> >2σ(<i>I</i>)]	0.0375/0.0646	0.0634/0.1454	0.0343/0.0616
<i>R</i> ₁ ^a / <i>wR</i> ₂ ^b (all data)	0.0618/0.0735	0.1044/0.1612	0.0568/0.0691
GOF on <i>F</i> ²	1.036	1.065	1.025

^a*R*₁ = Σ(||*F*₀| - |*F*_C|)/Σ|*F*₀|. ^b*wR*₂ = [Σ*w*(|*F*₀|² - |*F*_C|²)²/(Σ*w*|*F*₀|²)²]^{1/2}.

Table S2. Crystal data and structure refinements for **JXUST-41**, **JXUST-41a** and **JXUST-41b**

Compound	JXUST-41	JXUST-41a	JXUST-41b
formula	C ₇₈ H ₅₂ N ₁₀ O ₂₈ S ₃ Dy ₄	C ₆₆ H ₄₄ N ₆ O ₃₄ S ₃ Dy ₄	C ₇₈ H ₅₂ N ₁₀ O ₂₈ S ₃ Dy ₄
<i>M_r</i>	2323.47	2211.28	2323.47
<i>T</i> (K)	273(2)	293(2)	273(2)
crystal system	triclinic	triclinic	triclinic
space group	<i>P</i> ī	<i>P</i> ī	<i>P</i> ī
<i>a</i> (Å)	10. 9183(5)	10.9980 (12)	10.9883(5)
<i>b</i> (Å)	12.0025(6)	11.1805(13)	12.5025(6)
<i>c</i> (Å)	15.8371(6)	15.8136(17)	15.4371(6)
α (°)	73.454(10)	104.902(4)	73.354(10)
β (°)	70.816(10)	109.430(3)	70.616(10)
γ (°)	86.911(10)	90.228(4)	86.511(10)
<i>V</i> (Å ³)	1877.18(15)	1763.5(3)	1915.34(15)
<i>Z</i>	1	1	1
<i>F</i> (000)	1126	1066	1126
<i>D</i> _{calc} (g cm ⁻³)	2.055	2.082	2.014
μ (mm ⁻¹)	4.114	4.378	4.032
Collected reflections	23053	18642	23480
Unique reflections	6546	6110	6703
<i>R</i> _{int}	0.0265	0.0615	0.0269
<i>R</i> ₁ ^a / <i>wR</i> ₂ ^b [<i>I</i> >2σ(<i>I</i>)]	0.0244/0.0491	0.0657/0.1406	0.0293/0.0685
<i>R</i> ₁ ^a / <i>wR</i> ₂ ^b (all data)	0.0307/0.0511	0.1014/0.1619	0.0358/0.0711
GOF on <i>F</i> ²	1.067	1.052	1.091

^a*R*₁ = Σ(|*F*₀| - |*F*_C|)/Σ|*F*₀|. ^b*wR*₂ = [Σ*w*(|*F*₀|² - |*F*_C|²)²/(Σ*w*|*F*₀|²)²]^{1/2}.

Table S3. Selected bond lengths (Å) and angles (°) for **JXUST-40^a**

Gd1—O1	2.299(5)	Gd2—O13	2.340(5)
Gd1—O5 ⁱ	2.263(11)	Gd2—O6A ⁱⁱ	2.230(19)
Gd1—O7 ⁱⁱ	2.450(4)	Gd2—O2 ⁱⁱⁱ	2.304(4)
Gd1—O8 ⁱⁱ	2.422(4)	Gd2—O3	2.454(4)
Gd1—O11	2.434(14)	Gd2—O4	2.373(4)
Gd1—O12	2.367(5)	Gd2—O6 ⁱⁱ	2.350(18)
Gd1—O14	2.412(6)	O5 ⁱ —Gd1—O14	84.5(7)
O1—Gd1—O7 ⁱⁱ	77.40(17)	O8 ⁱⁱ —Gd1—O7 ⁱⁱ	53.26(15)
O1—Gd1—O8 ⁱⁱ	103.87(17)	O8 ⁱⁱ —Gd1—O11	116.7(4)
O1—Gd1—O11	98.9(5)	O11—Gd1—O7 ⁱⁱ	76.4(5)
O1—Gd1—O12	158.3(2)	O12—Gd1—O7 ⁱⁱ	118.24(16)
O1—Gd1—O14	84.1(2)	O12—Gd1—O8 ⁱⁱ	77.84(16)
O5 ⁱ —Gd1—O1	87.2(5)	O12—Gd1—O11	99.5(6)
O5 ⁱ —Gd1—O7 ⁱⁱ	147.2(6)	O12—Gd1—O14	74.8(2)
O5 ⁱ —Gd1—O8 ⁱⁱ	159.5(5)	O14—Gd1—O7 ⁱⁱ	121.7(2)
O5 ⁱ —Gd1—O11	77.7(8)	O14—Gd1—O8 ⁱⁱ	79.58(19)
O5 ⁱ —Gd1—O12	85.6(5)	O14—Gd1—O11	161.7(5)
O6 ⁱⁱ —Gd2—O4	114.5(5)	O2 ⁱⁱⁱ —Gd2—O3	145.10(16)
O13—Gd2—O3	80.65(17)	O2 ⁱⁱⁱ —Gd2—O4	158.69(16)
O13—Gd2—O4	105.17(18)	O2 ⁱⁱⁱ —Gd2—O6 ⁱⁱ	85.2(5)
O13—Gd2—O6 ⁱⁱ	104.1(5)	O2 ⁱⁱⁱ —Gd2—O13	75.75(17)
O4—Gd2—O3	53.45(15)	O6 ⁱⁱ —Gd2—O3	76.0(5)

^aSymmetry codes: (i) $x, y, z+1$; (ii) $x-1, y, z+1$; (iii) $x-1, y, z$; (iv) $x+1, y, z-1$.

Table S4. Selected bond lengths (\AA) and angles ($^\circ$) for **JXUST-40a^b**

Gd1—O1	2.38(3)	Gd1—O10 ⁱ	2.371(9)
Gd1—O1W	2.277(8)	Gd1—O11 ⁱⁱ	2.276(8)
Gd1—O5	2.264(10)	Gd2—O2W	2.309(8)
Gd1—O9 ⁱ	2.498(9)	Gd2—O7 ⁱⁱ	2.455(8)
Gd2—O3	2.59(4)	Gd2—O8 ⁱⁱ	2.410(10)
Gd2—O4	2.48(2)	Gd2—O12 ⁱⁱⁱ	2.241(8)
Gd2—O6 ⁱ	2.234(8)	O1W—Gd1—O1	78.4(7)
O1W—Gd1—O9 ⁱ	79.2(4)	O1—Gd1—O9 ⁱ	111.8(8)
O1W—Gd1—O10 ⁱ	107.4(4)	O5—Gd1—O1	170.1(8)
O5—Gd1—O9 ⁱ	73.7(3)	O5—Gd1—O1W	95.0(4)
O5—Gd1—O10 ⁱ	113.8(3)	O5—Gd1—O11 ⁱⁱ	88.1(3)
O10 ⁱ —Gd1—O1	75.5(8)	O10 ⁱ —Gd1—O9 ⁱ	52.3(3)
O11 ⁱⁱ —Gd1—O1	83.3(8)	O11 ⁱⁱ —Gd1—O9 ⁱ	149.0(3)
O11 ⁱⁱ —Gd1—O1W	77.6(4)	O11 ⁱⁱ —Gd1—O10 ⁱ	156.5(3)
O2W—Gd2—O3	123.5(8)	O2W—Gd2—O7 ⁱⁱ	118.7(4)
O2W—Gd2—O4	74.6(6)	O2W—Gd2—O8 ⁱⁱ	77.0(4)
O4—Gd2—O3	51.7(9)	O6 ⁱ —Gd2—O4	87.3(6)
O6 ⁱ —Gd2—O2W	82.1(4)	O6 ⁱ —Gd2—O7 ⁱⁱ	152.1(4)
O6 ⁱ —Gd2—O8 ⁱⁱ	154.4(4)	O7 ⁱⁱ —Gd2—O3	76.7(9)
O6 ⁱ —Gd2—O12 ⁱⁱⁱ	90.7(3)	O7 ⁱⁱ —Gd2—O4	115.0(6)
O8 ⁱⁱ —Gd2—O3	72.2(9)	O12 ⁱⁱⁱ —Gd2—O3	152.2(9)
O8 ⁱⁱ —Gd2—O4	73.1(6)	O12 ⁱⁱⁱ —Gd2—O4	152.3(6)
O8 ⁱⁱ —Gd2—O7 ⁱⁱ	53.5(3)	O12 ⁱⁱⁱ —Gd2—O7 ⁱⁱ	77.1(3)
O12 ⁱⁱⁱ —Gd2—O2W	77.8(4)	O12 ⁱⁱⁱ —Gd2—O8 ⁱⁱ	99.0(4)

^bSymmetry codes: (i) $x, y, z+1$; (ii) $x+1, y, z+1$; (iii) $x+1, y, z+2$.

Table S5. Selected bond lengths (\AA) and angles ($^{\circ}$) for **JXUST-40b^c**

Gd1—O8 ⁱⁱ	2.416(4)	Gd1—O14	2.260(6)
Gd1—O11	2.114(5)	Gd2—O2 ⁱⁱⁱ	2.307(4)
Gd1—O12	2.390(5)	Gd2—O3	2.438(4)
O8 ⁱⁱ —Gd1—O7 ⁱⁱ	52.18(15)	O14—Gd1—O5 ⁱ	78.8(2)
O11—Gd1—O5 ⁱ	79.2(2)	O14—Gd1—O7 ⁱⁱ	122.2(2)
O11—Gd1—O7 ⁱⁱ	79.21(19)	O14—Gd1—O8 ⁱⁱ	81.7(2)
O11—Gd1—O8 ⁱⁱ	119.11(18)	O14—Gd1—O12	74.4(2)
O11—Gd1—O14	157.9(2)	O2 ⁱⁱⁱ —Gd2—O4	158.57(16)
O12—Gd1—O7 ⁱⁱ	117.56(16)	O2 ⁱⁱⁱ —Gd2—O6 ⁱⁱ	83.55(15)
O12—Gd1—O8 ⁱⁱ	76.88(17)	O2 ⁱⁱⁱ —Gd2—O9 ^{iv}	86.25(15)
O10 ⁱⁱⁱ —Gd2—O6 ⁱⁱ	90.19(17)	O4—Gd2—O3	53.65(15)
O10 ⁱⁱⁱ —Gd2—O9 ^{iv}	86.64(16)	O6 ⁱⁱ —Gd2—O3	74.38(15)
O10 ⁱⁱⁱ —Gd2—O13	154.57(18)	O6 ⁱⁱ —Gd2—O4	116.90(16)
O13—Gd2—O2 ⁱⁱⁱ	75.52(18)	O6 ⁱⁱ —Gd2—O9 ^{iv}	169.65(14)
O13—Gd2—O3	81.75(18)	O9 ^{iv} —Gd2—O3	115.48(15)
O13—Gd2—O4	105.58(19)	O9 ^{iv} —Gd2—O4	73.05(15)
O13—Gd2—O6 ⁱⁱ	98.76(19)	O10 ⁱⁱⁱ —Gd2—O2 ⁱⁱⁱ	81.97(16)
O13—Gd2—O9 ^{iv}	80.31(18)	O10 ⁱⁱⁱ —Gd2—O3	123.65(17)

^cSymmetry codes: (i) $x, y, z+1$; (ii) $x-1, y, z+1$; (iii) $x-1, y, z$; (iv) $-x, -y+1, -z+1$;

Table S6. Selected bond lengths (\AA) and angles ($^\circ$) for **JXUST-41^d**

Dy1—O2 ⁱ	2.269(3)	Dy1—O17	2.312(19)
Dy1—O6 ⁱⁱ	2.275(3)	Dy2—O5	2.268(3)
Dy1—O7	2.434(3)	Dy2—O14	2.380(4)
Dy1—O8	2.341(3)	Dy1—O13	2.317(3)
Dy1—O11 ⁱⁱⁱ	2.17(2)	O2 ⁱ —Dy1—O6 ⁱⁱ	84.76(10)
O11 ⁱⁱⁱ —Dy1—O7	127.6(5)	O2 ⁱ —Dy1—O7	74.58(10)
O11 ⁱⁱⁱ —Dy1—O8	91.6(6)	O2 ⁱ —Dy1—O8	114.72(11)
O11 ⁱⁱⁱ —Dy1—O13	152.4(5)	O2 ⁱ —Dy1—O13	100.99(12)
O11 ⁱⁱⁱ —Dy1—O17	7.8(10)	O2 ⁱ —Dy1—O17	85.7(5)
O13—Dy1—O7	80.00(12)	O6 ⁱⁱ —Dy1—O7	144.54(11)
O13—Dy1—O8	106.23(12)	O6 ⁱⁱ —Dy1—O8	158.92(10)
O17—Dy1—O7	120.0(5)	O6 ⁱⁱ —Dy1—O13	75.99(12)
O17—Dy1—O8	87.5(5)	O6 ⁱⁱ —Dy1—O17	86.0(5)
O17—Dy1—O13	160.0(5)	O8—Dy1—O7	54.28(10)
O5—Dy2—O14	85.25(14)	O11 ⁱⁱⁱ —Dy1—O2 ⁱ	90.0(6)
O11 ⁱⁱⁱ —Dy1—O6 ⁱⁱ	79.9(6)		

^dSymmetry codes: (i) $x+1, y, z-1$; (ii) $x+1, y, z$; (iii) $-x+2, -y, -z+1$.

Table S7. Selected bond lengths (Å) and angles (°) for **JXUST-41a^e**

Dy1—O2	2.255(9)	Dy1—O5 ⁱ	2.257(10)
Dy1—O2W	2.340(15)	Dy1—O7 ⁱⁱ	2.498(11)
Dy2—O1	2.193(10)	Dy1—O8 ⁱⁱ	2.356(10)
Dy2—O1W	2.222(9)	Dy1—O9	2.33(3)
Dy2—O3 ^{iv}	2.431(10)	Dy1—O13 ⁱⁱⁱ	2.26(2)
Dy2—O4 ^{iv}	2.408(10)	O2—Dy1—O2W	95.0(5)
Dy2—O6 ⁱ	2.217(9)	O2—Dy1—O5 ⁱ	87.6(4)
Dy2—O11	2.48(3)	O2—Dy1—O7 ⁱⁱ	73.3(4)
O2—Dy1—O9	87.7(7)	O2—Dy1—O8 ⁱⁱ	113.5(4)
O2—Dy1—O13 ⁱⁱⁱ	171.0(6)	O2W—Dy1—O7 ⁱⁱ	78.3(5)
O5 ⁱ —Dy1—O2W	77.9(5)	O2W—Dy1—O8 ⁱⁱ	107.4(4)
O5 ⁱ —Dy1—O9	85.7(7)	O5 ⁱ —Dy1—O7 ⁱⁱ	147.9(4)
O8 ⁱⁱ —Dy1—O7 ⁱⁱ	52.9(4)	O5 ⁱ —Dy1—O8 ⁱⁱ	157.1(4)
O9—Dy1—O2W	163.2(7)	O9—Dy1—O7 ⁱⁱ	118.2(7)
O13 ⁱⁱⁱ —Dy1—O2W	89.4(6)	O9—Dy1—O8 ⁱⁱ	86.5(7)
O13 ⁱⁱⁱ —Dy1—O9	85.9(8)	O13 ⁱⁱⁱ —Dy1—O5 ⁱ	85.6(6)
O1—Dy2—O1W	72.5(4)	O13 ⁱⁱⁱ —Dy1—O7 ⁱⁱ	115.3(6)
O1—Dy2—O3 ^{iv}	153.7(4)	O13 ⁱⁱⁱ —Dy1—O8 ⁱⁱ	72.4(6)
O1—Dy2—O4 ^{iv}	152.2(4)	O1W—Dy2—O3 ^{iv}	124.6(5)
O1—Dy2—O6 ⁱ	89.6(4)	O1W—Dy2—O4 ^{iv}	83.5(4)
O1—Dy2—O11	82.1(7)	O1W—Dy2—O11	153.0(7)
O4 ^{iv} —Dy2—O3 ^{iv}	53.7(4)	O3 ^{iv} —Dy2—O11	76.5(7)
O4 ^{iv} —Dy2—O11	123.4(7)	O6 ⁱ —Dy2—O3 ^{iv}	76.7(4)
O6 ⁱ —Dy2—O1W	77.5(5)	O6 ⁱ —Dy2—O4 ^{iv}	98.7(4)
O6 ⁱ —Dy2—O11	93.6(7)		

^eSymmetry codes: (i) $x+1, y, z+1$; (ii) $x, y, z+1$; (iii) $x-1, y-1, z$; (iv) $x+1, y, z$.

Table S8. Selected bond lengths(Å) and angles(°) for **JXUST-41b^f**

Gd1—O8 ⁱ	2.269(4)	Gd2—O1 ⁱⁱⁱ	2.307(4)
Gd1—O12 ⁱⁱ	2.432(4)	Gd2—O4	2.438(4)
Gd1—O9	1.948(17)	Gd2—O6	2.398(4)
Gd1—O5	2.389(4)	Gd2—O10 ⁱⁱ	2.309(4)
Gd1—O3	2.304(5)	Gd2—O11	2.182(4)
Gd1—O13	2.261(6)	O8 ⁱ —Gd1—O12 ⁱⁱ	150.56(16)
O8 ⁱ —Gd1—O3	84.62(16)	O8 ⁱ —Gd1—O5	86.34(16)
O9—Gd1—O8 ⁱ	79.0(6)	O5—Gd1—O12 ⁱⁱ	117.52(16)
O9—Gd1—O12 ⁱⁱ	77.5(6)	O3—Gd1—O12 ⁱⁱ	77.29(16)
O9—Gd1—O5	107.4(5)	O3—Gd1—O5	159.96(18)
O9—Gd1—O3	88.4(5)	O9—Gd1—O13	157.6(6)
O13—Gd1—O8 ⁱ	78.9(2)	O13—Gd1—O5	74.4(2)
O13—Gd1—O12 ⁱⁱ	122.2(2)	O13—Gd1—O3	86.3(2)
O1 ⁱⁱⁱ —Gd2—O4	145.46(15)	O6—Gd2—O4	53.53(14)
O1 ⁱⁱⁱ —Gd2—O6	158.58(15)	O10 ⁱⁱ —Gd2—O4	74.43(14)
O1 ⁱⁱⁱ —Gd2—O10 ⁱⁱ	83.58(14)	O10 ⁱⁱ —Gd2—O6	116.87(15)
O11—Gd2—O1 ⁱⁱⁱ	75.63(17)	O11—Gd2—O6	105.49(18)
O11—Gd2—O4	81.69(17)	O11—Gd2—O10 ⁱⁱ	98.73(18)

^fSymmetry codes: (i) $x+1, y, z-1$; (ii) $x+1, y, z$; (iii) $x-1, y+1, z$.

Table S9. SHAPE analysis of the Gd^{III} ions in **JXUST-40**

Ions	Label	Shape	Symmetry	Distortion (τ)
	HP-7	Heptagon	D_{7h}	29.478
	HPY-7	Hexagonal pyramid	C_{6v}	19.495
	PBPY-7	Pentagonal bipyramid	D_{5h}	5.023
Gd1	CO-C-7	Capped octahedron	C_{3v}	2.510
	CTPR-7	Capped trigonal prism	C_{2v}	1.858
	JPBPY-7	Johnson pentagonal bipyramid J13	D_{5h}	8.322
	JETPY-7	Johnson elongated triangular pyramid J7	C_{3v}	16.540
	HP-7	Heptagon	D_{7h}	33.217
	HPY-7	Hexagonal pyramid	C_{6v}	19.430
	PBPY-7	Pentagonal bipyramid	D_{5h}	6.190
Gd2	CO-C-7	Capped octahedron	C_{3v}	1.988
	CTPR-7	Capped trigonal prism	C_{2v}	1.794
	JPBPY-7	Johnson pentagonal bipyramid J13	D_{5h}	9.400
	JETPY-7	Johnson elongated triangular pyramid J7	C_{3v}	18.228

Table S10. SHAPE analysis of the Gd^{III} ions in **JXUST-40a**

ions	label	Shape	symmetry	distortion(τ)
Gd1	HP-7	Heptagon	D_{7h}	31.882
	HPY-7	Hexagonal pyramid	C_{6v}	20.265
	PBPY-7	Pentagonal bipyramid	D_{5h}	6.091
	COC-7	Capped octahedron	C_{3v}	2.508
	CTPR-7	Capped trigonal prism	C_{2v}	1.501
	JPBPY-7	Johnson pentagonal bipyramid J13	D_{5h}	9.392
	JETPY-7	Johnson elongated triangular pyramid J7	C_{3v}	17.531
Gd2	OP-8	Octagon	D_{8h}	33.514
	HPY-8	Heptagonal pyramid	C_{7v}	21.895
	HBPY-8	Hexagonal bipyramid	D_{6h}	15.247
	CU-8	Cube	O_h	10.301
	SAPR-8	Square antiprism	D_{4d}	2.340
	TDD-8	Triangular dodecahedron	D_{2d}	3.084
	JGBF-8	Johnson gyrobifastigium J26	D_{2d}	14.003
	JETBPY-8	Johnson elongated triangular bipyramid J14	D_{3h}	28.586

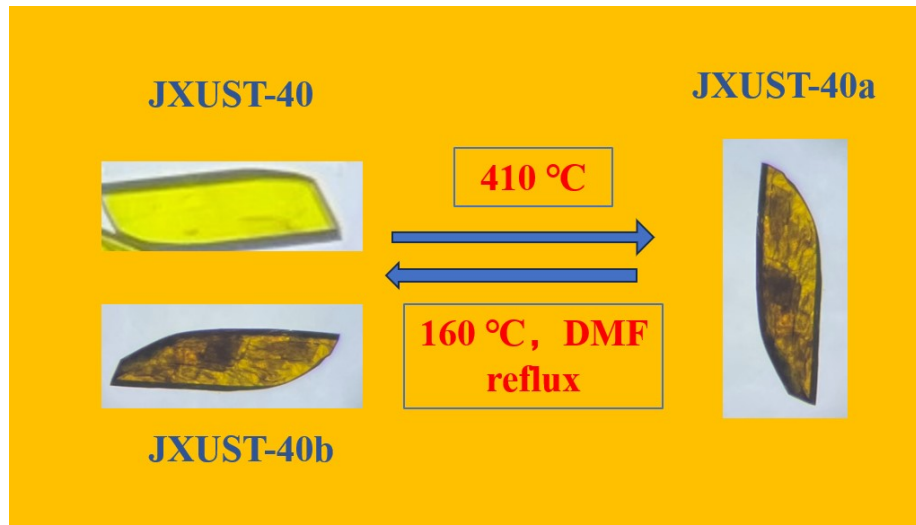


Fig. S1 Schematic diagram of the reversible transformation of **JXUST-40**, **JXUST-40a** and **JXUST-40b**

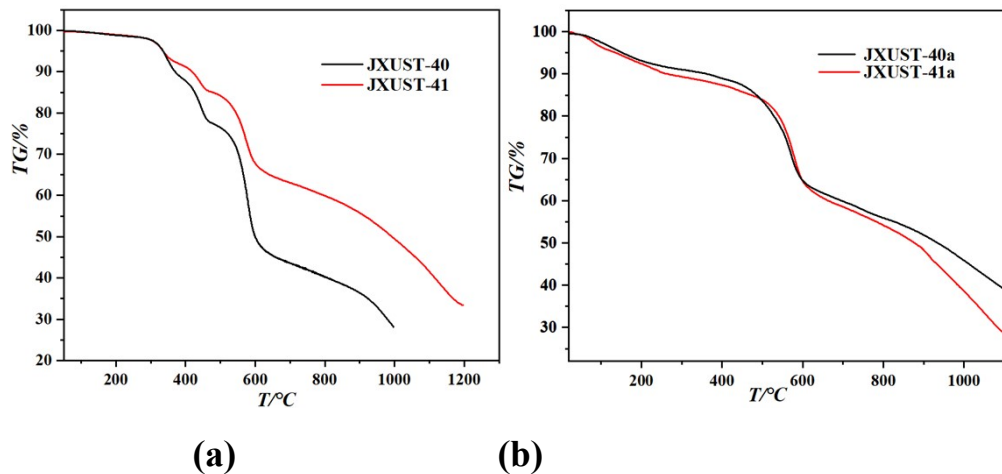
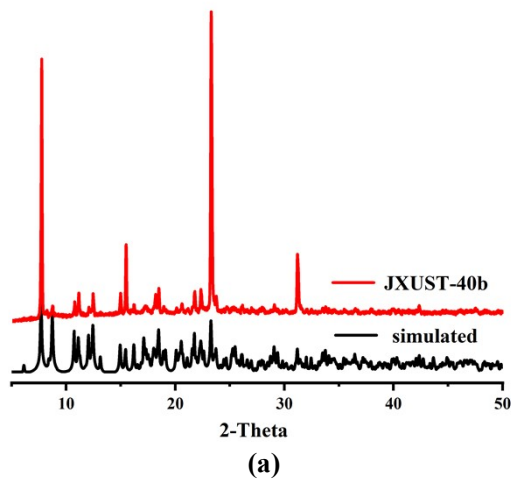
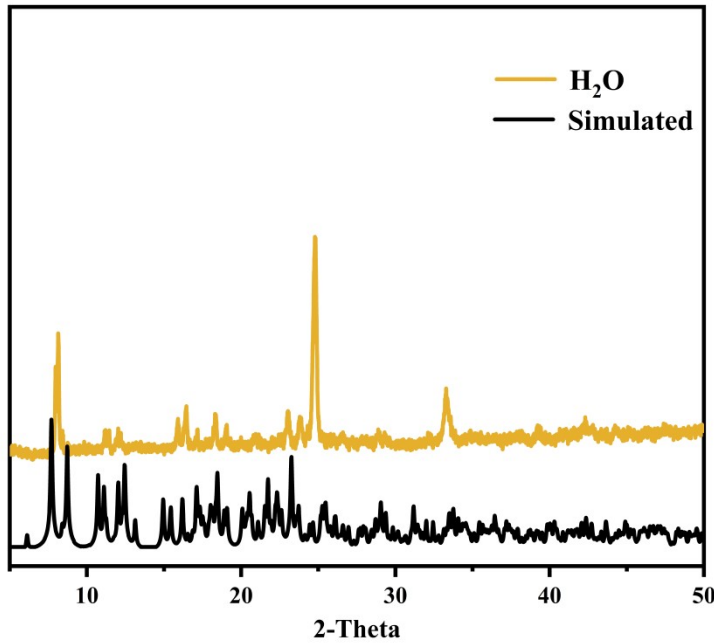


Fig. S2 (a) The TGA curves for **JXUST-40** and **JXUST-41**; (b) The TGA curves for **JXUST-40a** and **JXUST-41a**.





(b)

Fig. S3 (a) The simulated and experimental PXRD patterns of **JXUST-40b**; (b) the simulated and experimental PXRD patterns of **JXUST-40** soaked in aqueous solution for 24 h.

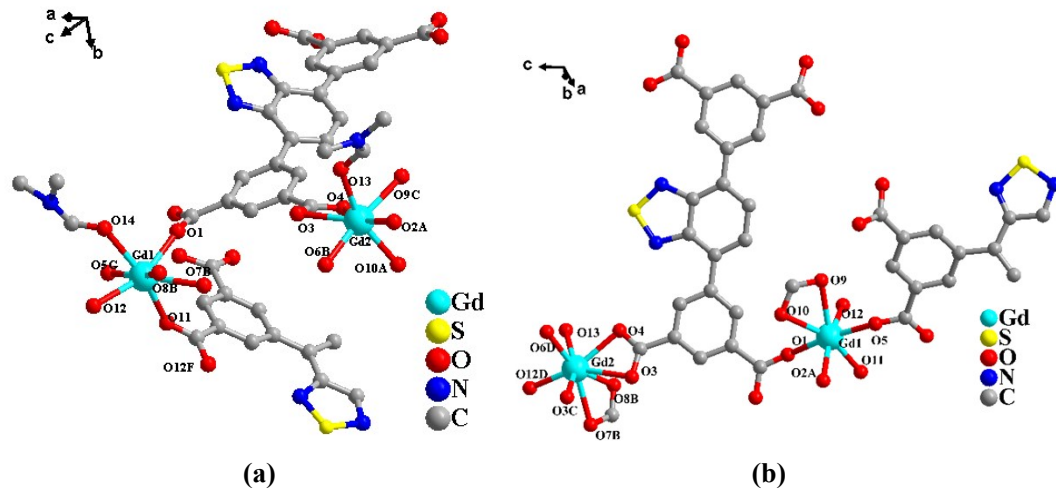


Fig. S4 (a) Ball-and-stick view of the coordination environments of Gd^{III} in **JXUST-40** (symmetry codes: A: $x, y, z+1$; B: $x-1, y, z+1$; C: $-x, -y+1, -z+2$; D: $x-1, y, z$); (b) Ball-and-stick view of the coordination environments of Gd^{III} in **JXUST-40a** (symmetry codes: A: $-x+1, -y+1, -z+2$; B: $-x+1, -y+1, -z+3$; C: $x, y, z+1$; D: $x+1, y, z+1$).

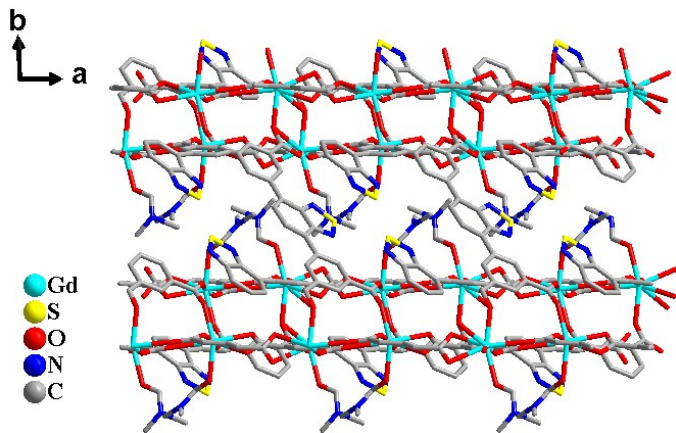


Fig. S5 View of the 3D structure of **JXUST-40** along the *c* axis.

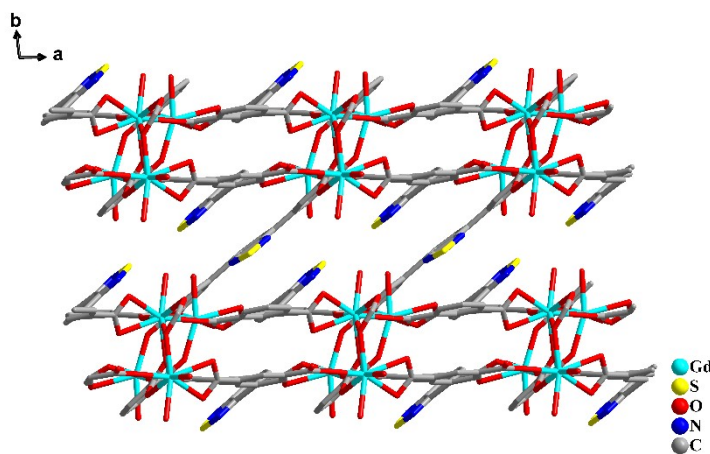
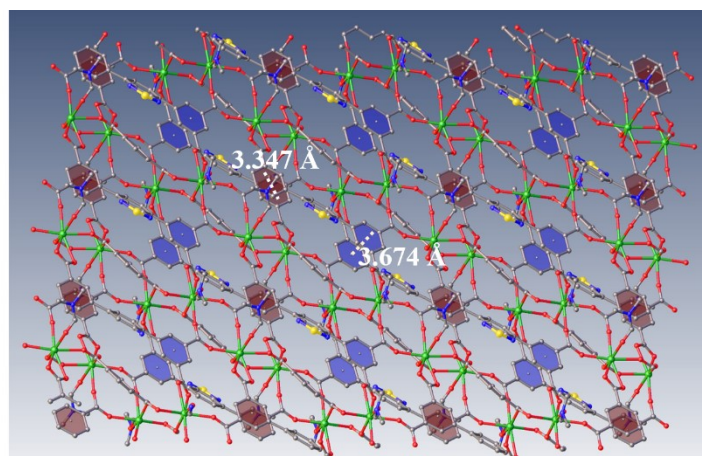
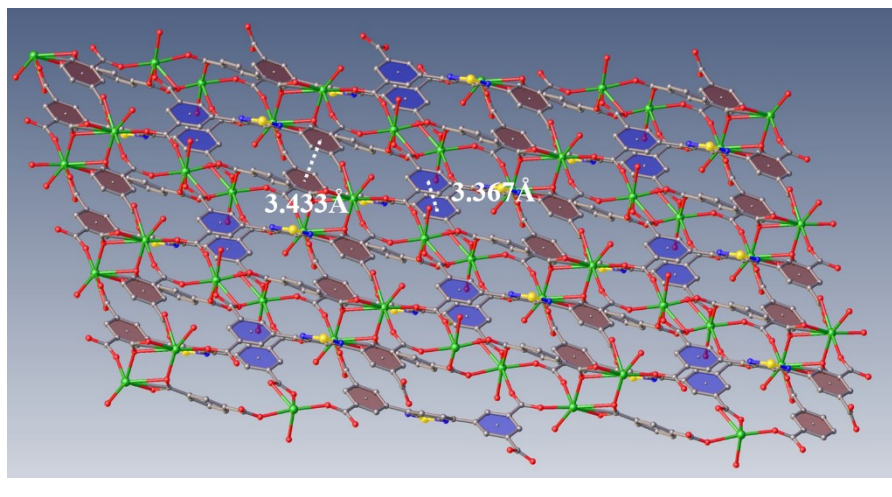


Fig. S6 View of the 3D structure of **JXUST-40a** along the *c* axis



(a)



(b)

Fig. S7 The $\pi\cdots\pi$ stacking structures of (a) JXUST-40 and (b) JXUST-40a.

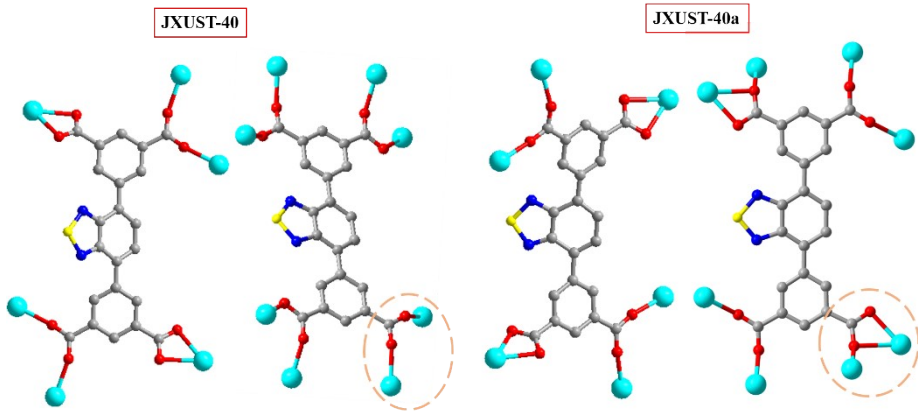


Fig. S8 The coordination modes of BTDI^{4-} ligands in JXUST-40 and JXUST-40a.

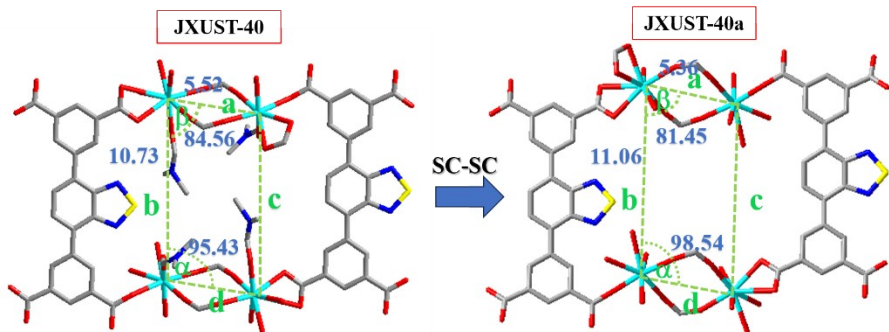


Fig. S9 Variation in bond lengths and angles of the edges of a parallelogram for JXUST-40 and JXUST-40a.

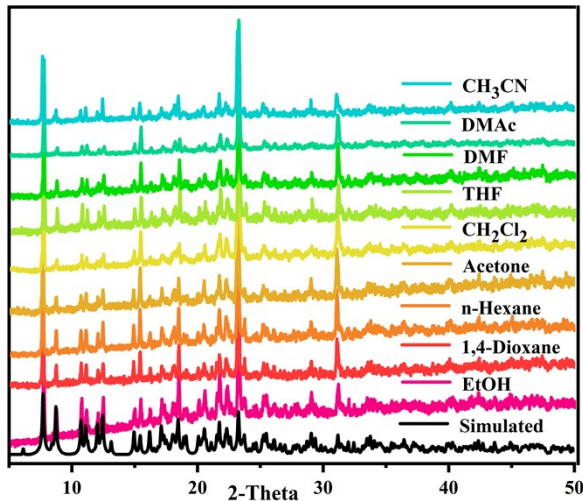


Fig. S10 The experimental PXRD patterns of **JXUST-40** soaked in common solvents.

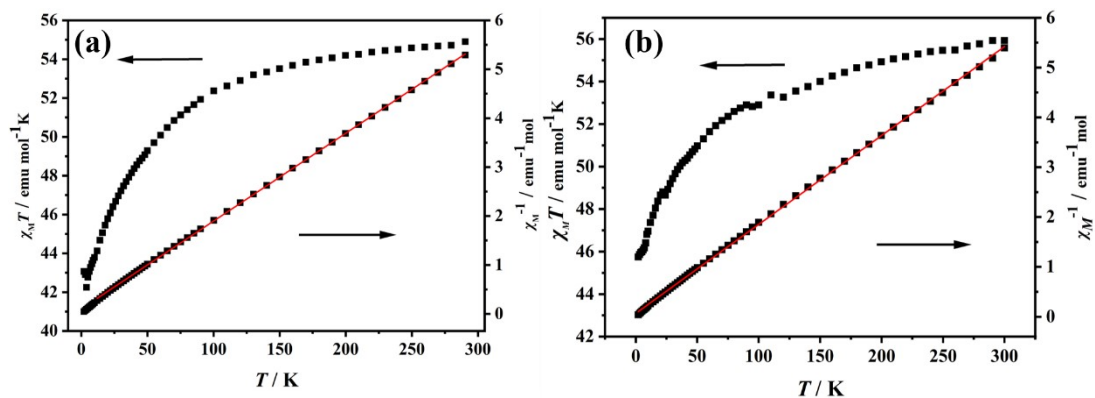


Fig. S11 Temperature dependencies of the magnetic susceptibility product ($\chi_M T$) at 2–300 K with a dc field of 1 kOe for (a) **JXUST-41** and (b) **JXUST-41a**.

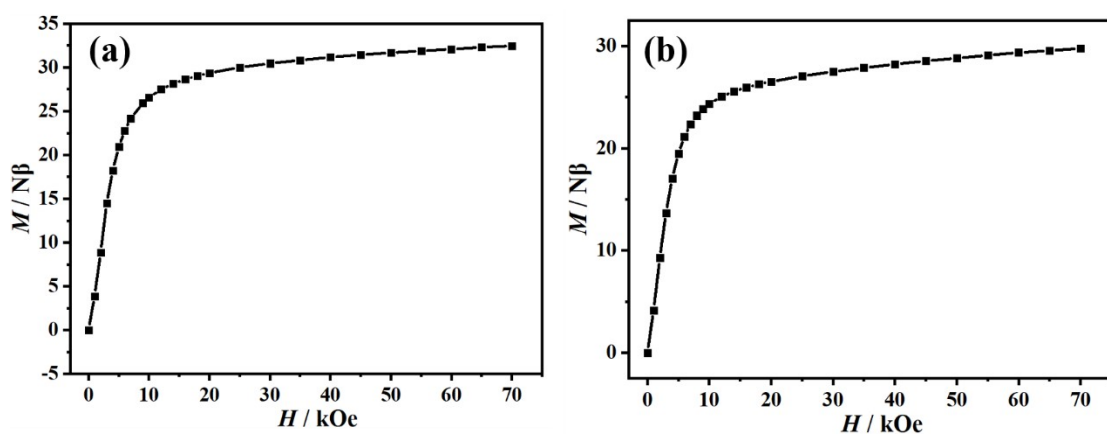


Fig. S12 The M – H plots at 2 K for (a) **JXUST-41** and (b) **JXUST-41a**.

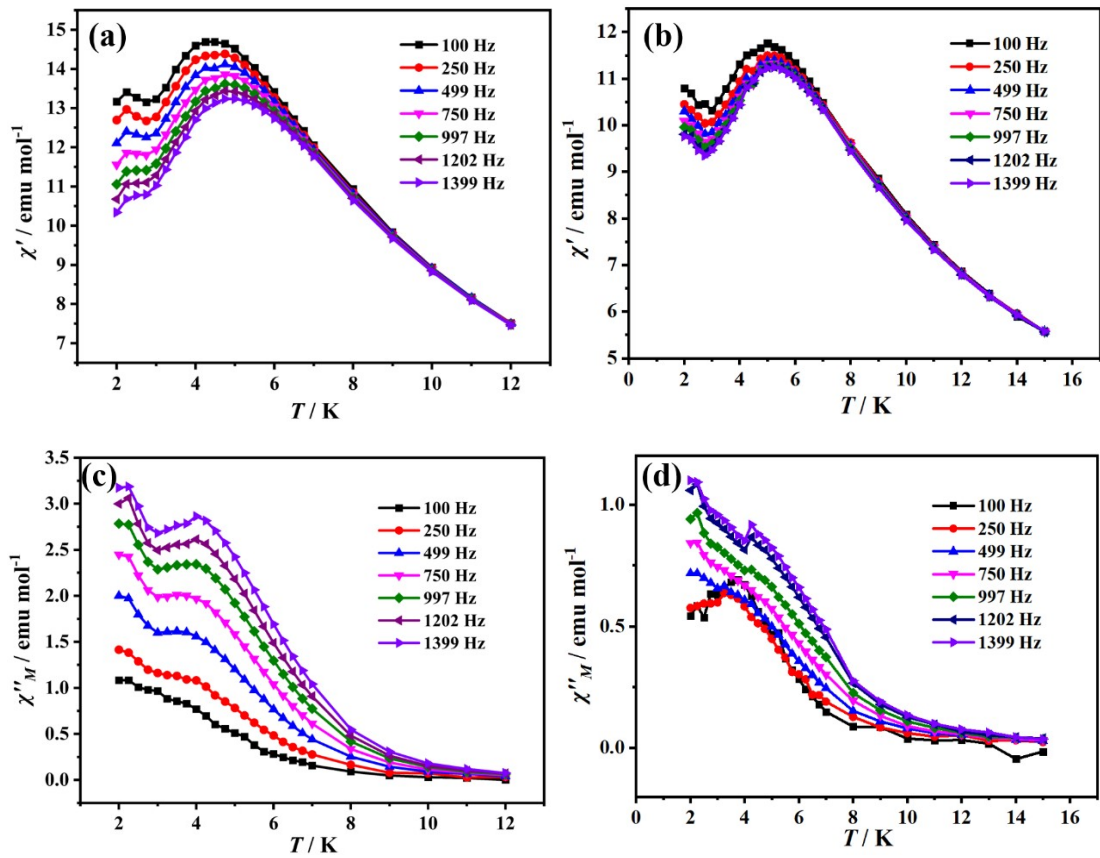


Fig. S13 Temperature dependence of the in-phase (χ') and out-of-phase (χ'') ac susceptibilities measured at varying frequencies under 2 kOe dc field for (a, c) JXUST-41 and (b, d) JXUST-41a.